Vanadium oxide nanowires for Li-ion batteries

Liqiang Mai[a)]
State Key Laboratory of Advanced Technology for Materials Synthesis and Processing, Wuhan University of Technology, Wuhan 430070, People's Republic of China; and Department of Chemistry and Chemical Biology, Harvard University, Cambridge, Massachusetts 02138

Xu Xu, Lin Xu, Chunhua Han, and Yanzhu Luo
State Key Laboratory of Advanced Technology for Materials Synthesis and Processing, Wuhan University of Technology, Wuhan 430070, People's Republic of China

(Received 25 January 2011; accepted 18 April 2011)

Vanadium oxide nanowires have gained increasing interest as the electrode materials for Li-ion batteries. This article presents the recent developments of vanadium oxide nanowire materials and devices in Li-ion batteries. First, we will describe synthesis and construction of vanadium oxide nanowires. Then, we mainly focus on the electrochemical performances of vanadium oxide nanowires, such as VO_2, V_2O_5, hydrated vanadium oxides, LiV_3O_8, silver vanadium oxides, etc. Moreover, design and in situ characterization of the single nanowire electrochemical device are also discussed. The challenges and opportunities of vanadium oxide nanowire electrode materials will be discussed as a conclusion to push the fundamental and practical limitations of this kind of nanowire materials for Li-ion batteries.

I. INTRODUCTION

Li-ion batteries for portable electronic devices and hybrid electric vehicles have gained great importance for energy storage today.[1–3] However, how to prepare cathode materials with higher energy density, higher potential, and longer cycle life is still a challenge. Vanadium oxides have interesting open-layered structures, which permit a wide variety of other molecules or cations to intercalate into the layers. In Li-ion batteries, these open-layered structures can host more Li ions to lead to higher specific capacity than commercial $LiCoO_2$ with an anion close packed lattice. Taking V_2O_5, for example, the apices of these pyramids alternate in an up-up-down-down sequence with every third row being vacant, forming a layered character for the V_2O_5 structure,[4] providing the accommodating interlayer space for the intercalation reactions that are the conventional mechanism in all consumer rechargeable batteries. The intercalation of Li ion into the V_2O_5 interlayer space causes the formation of $Li_xV_2O_5$ phase, which would not change the original structural frameworks, and the intercalation process is still fully reversible, leading to the advantage of the Li-ion batteries with a high output voltage.[5] Vanadium sources are known to be abundant in the crustal rock of earth, causing the low cost, which is another advantage of vanadium oxides compared with $LiCoO_2$ with high price because of the relatively limited source of Co.[6] These advantages make vanadium oxides such as V_2O_5, VO_2, hydrated vanadium oxides, silver vanadium oxides (SVO), LiV_3O_8, etc. receive much attention for application in Li-ion battery. However, vanadium oxides are limited by fast capacity fading because of a decrease of the Li diffusion coefficient D_{Li} and low electrical conductivity at the state of discharge.

Since oxide nanorods were produced by Yang and Lieber[7] in 1996, oxide nanorods and nanowires have received great interest. Recently, oxide nanowire electrodes are found to present excellent cycling performance because of their high surface area, short Li-ion diffusion distances, and facile strain relaxation on electrochemical cycling.[8–10] Vanadium oxides as cathode materials have been investigated since 1976,[11] and to date, several review articles summarizing the application of vanadium oxide nanomaterials in Li-ion batteries have already been reported by Whittingham and coworkers[12], Wang and Cao[13], and Wu and Xie[14]. But there is no review that systematically summarizes the synthesis, construction, battery property, and device assembly of vanadium oxide nanowires. Here, we mainly review some typical vanadium oxides nanowires, such as VO_2, V_2O_5, hydrated vanadium oxides, etc. from synthesis and construction to battery property and device assembly based on the recent advance and our group's studies.

II. SYNTHESIS AND CONSTRUCTION OF VANADIUM OXIDE NANOWIRES

Several conventional methods are usually applied to synthesize vanadium oxide nanowires and other nanostructures, such as hydrothermal, chemical vapor deposition

[a)]Address all correspondence to this author.
e-mail: mlq@cmliris.harvard.edu
DOI: 10.1557/jmr.2011.171

(CVD), template assisted, etc. Figures 1(a)–1(c) are the typical scanning electron microscopic images of vanadium oxide nanowires synthesized by hydrothermal,[15] CVD,[16] and template-assisted method,[17] respectively. In this article, we will just review some novel synthesis methods of vanadium oxide nanowires in recent years. Cheng et al.[18] have described interesting growth behaviors of VO_2 single-crystalline nanowires on silica substrate surfaces without using any metal catalysts. The VO_2 nanowires produced by self-catalytic growth showed that vanadium oxide materials at the tips and nanowire bodies have different melting temperatures, and the growth of VO_2 nanowires is oxide assisted. Velazquez et al.[19] prepared V_2O_5 nanowires arrays on silicon substrates by thermal evaporation method. The nanowires obtained are single crystalline and highly oriented with their lengths and substrate coverage controlled by the duration of the reaction, reaction temperature, and flow velocity. The growth of these nanowire arrays has great value in the fabrication of novel battery architectures based on the individual nanowire. Vertically aligned V_2O_5 nanowires on an indium tin oxide surface were prepared by vapor transport,[20] and this method combines gaseous transport and pyrolytic deposition of vanadium polyoxometalate anions and yields vertically aligned vanadium oxide nanowires [Fig. 1(d)]. Liu and coworkers[21] introduced a facile thermal decomposition method in the fabrication of V_2O_5 nanorods [Fig. 1(e)], and the electrochemical performance of V_2O_5 nanorods is much better than commercial V_2O_5. The transformation from V_2O_5 powders to nanorods has been realized via a two-step approach by Glushenkov et al.[22] The V_2O_5 powders were obtained by a ball milling treatment, and the nanorods were formed through a controlled nanoscale growth from the V_2O_5 powders. The results show that the crystal orientation of nanorods provides an improved cycling stability for Li intercalation. A V_2O_5 nanobelt array was designed and prepared on a conductive substrate via a wet-chemistry approach by Wang et al.[23] The synthesis strategy is based on the action of hydrogen bonding between the functionalized surface of a Ti substrate and the earlier-formed $V_2O_5.xH_2O$ nanoseeds, and then the nanobelts are motivated and evolved from the nanoseeds mentioned above. The as-prepared V_2O_5 nanobelt array exhibits a greatly enhanced performance in Li-ion batteries as the cathode and anode with respect to the rate capability, stability, and cyclability.

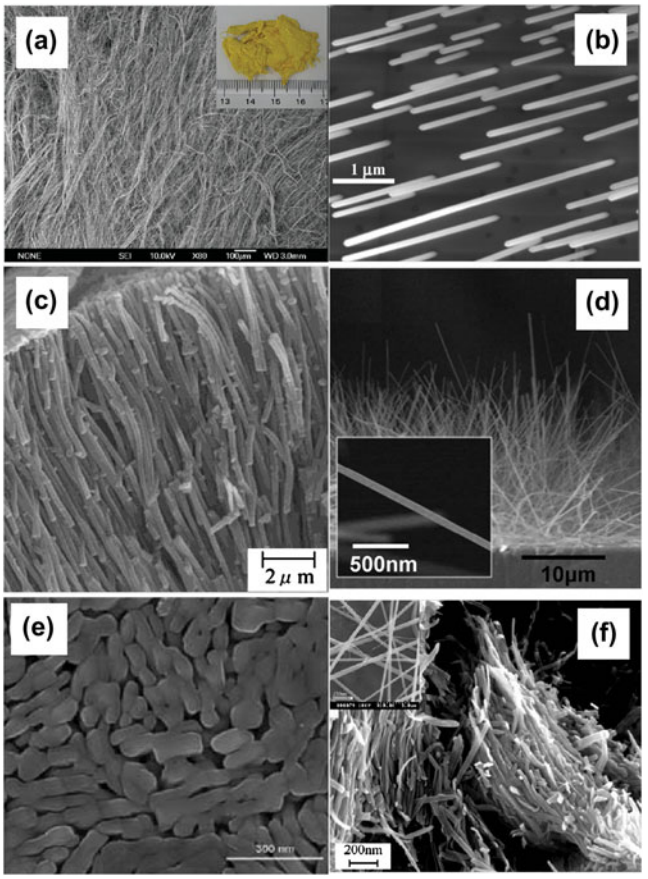

FIG. 1. Scanning electron microscope (SEM) images of vanadium oxide nanowires or nanorods synthesized by different methods. (a) Hydrothermal.[15] (b) CVD.[16] (c) Template assisted.[17] (d) Vapor transport.[20] (e) Thermal decomposition.[21] (f) Electrospinning combined with hydrothermal.[25]

Electrospinning has been widely used as a convenient and versatile method for preparing ultralong nanowires with controllable lengths, diameters, compositions, and complex architectures. There has been much interest in electrospinning of vanadium oxide nanowires because nanostructured vanadium oxides with a typical layered structure have the potential to offer high capacities for Li-ion batteries. Whittingham and coworkers[24,25] synthesized vanadium oxide nanofibers by electrospinning technique combined with the hydrothermal method. The organic vanadium precursor was dissolved into a polymethylmethacrylate (PMMA) chloroform solution. The composite fibers were formed on the aluminum foil collector surface after the solvent evaporated and then heated with water in a Teflon-lined autoclave. The product was filtered, washed, and then dried. All residual organics were removed by Soxhlet extraction to obtain single crystal $H_xV_4O_{10}{\cdot}nH_2O$ nanofibers [Fig. 1(f)]. The crystallinity and morphology were maintained on heating to 500 °C when V_2O_5 was formed. Viswanathamurthi et al.[26] have synthesized vanadium oxide nanofibers by electrospinning. Sol–gel method was used to prepare the electrospinning solution with organic vanadium precursor. On applying a high voltage, the solvent evaporated, and a charged fiber was deposited on the collector in the form of a nonwoven fabric. The fibers were collected and then calcined at different temperatures from 400 to 700 °C to obtain V_2O_5 naonfibers. Cao and coworkers [27] applied a simple and environmentally benign method combining sol–gel processing with electrospinning followed by annealing in air for the fabrication of mesoporous V_2O_5 nanofibers. The resultant nanofibers are

350 nm in diameter and consist of porous polycrystalline vanadium oxide with a specific surface area of about 97 m^2/g. Such mesoporous V_2O_5 nanofibers allow easy mass and charge transfer with sufficient freedom for volume change accompanying the Li ion intercalation and deintercalation.

Recently, our group has designed and synthesized ultralong hierarchical vanadium oxide nanowires using the low-cost starting materials by electrospinning combined with annealing.[28] NH_4VO_3 was added to the 10 wt% aqueous poly(vinyl alcohol) (PVA) solution first. After the mixture was stirred at 70 °C for 3 h, a viscous light-yellow clear solution of ammonium metavanadate/PVA was obtained. The precursor solution was then delivered into a metallic needle at a constant flow rate of 1.0 mL/h by a computer controlled syringe pump. The metallic needle was connected to a high-voltage power supply, and a piece of grounded aluminum foil was placed 20 cm below the tip of the needle. As a high voltage of 20 kV was applied, the precursor solution jet accelerated toward the aluminum foil, leading to the formation of NH_4VO_3/PVA composite nanowires accompanied by rapid evaporation of solvent. The length of the nanowires can reach the millimeter or centimeter grade. Each individual nanowire is uniform in cross-section, with an average diameter of 200–250 nm. Interestingly, short nanorods of diameter of about 50 nm and length of 100 nm are grown on the surface of the nanowires [Fig. 2(a)], which is quite different from that in the literature on electrospinning of vanadium oxide nanowires from vanadium oxide isopropoxide.[26] The electrospun composite nanowires were then annealed at 480 °C in air for 3 h to obtain vanadium oxide nanowires. After annealing, the nanowires can remain long as the continuous structures, while the diameter decreases to 100–200 nm. Notably, it is found that the ultralong vanadium oxide nanowires are constructed from attached nanorods of diameter of approximately 50 nm and length of 100 nm [Fig. 2(b)]. From the transmission electron microscopic image [Fig. 2(c)], we can see that the nanorods are tightly attached with each other to construct the nanowires. Figure 2(d) shows lattice fringes of a nanorod with regular spacing of 4.38 and 3.48 Å, which are consistent with the interplanar distance of (001) and (201) planes of V_2O_5. The well-resolved fringes confirm the local single crystallinity of the V_2O_5 nanorods, which is in accordance with the corresponding fast Fourier transformation patterns shown in Fig. 2(e).

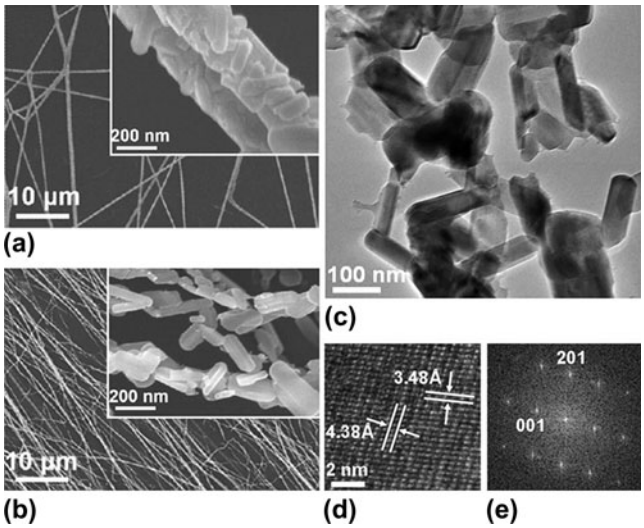

FIG. 2. (a) Field-emission scanning electron microscopic (FESEM) images of electrospun composite nanowires before annealing. (b) FESEM images of the ultralong hierarchical V_2O_5 nanowires after annealing. (c) Transmission electron microscopic (TEM) image of the ultralong hierarchical V_2O_5 nanowires after annealing. (d) High-resolution transmission electron microscope image and (e) fast Fourier transformation pattern of a single nanorod on the hierarchical V_2O_5 nanowires.[28]

Although nanowires have the potentials for various novel applications, organizing these nanoscale building blocks into assemblies and useful systems ultimately is still a challenge. To this end, Langmuir-Blodgett (LB) technique is an attractive methodology, because it can readily help to assemble one-dimensional nanostructures into large-area ordered monolayer arrays at the air–water interface.[29,30] Recently, our group reported the stable surface functionalization and LB assembly of VO_2 nanowires.[31] Briefly, the VO_2 nanowires with 30–60 nm in diameter and 1–5 μm in length were first prepared via a hydrothermal method as described previously.[32] To facilitate assembly, VO_2 nanowires were functionalized with steric acid (SA) in toluene, followed by cetyltrimethylammonium bromide (CTAB), centrifuged, and then resuspended in chloroform. The chloroform VO_2 nanowire suspension was spread dropwise on the aqueous phase of a LB trough. VO_2 nanowires were transferred using hydrophilic glass by a vertical dipping method to obtain final LB film. The x-ray diffraction (XRD) pattern of VO_2 nanowire LB films (Fig. 3) only exhibits (00l) peaks, while diffraction peak characteristic of other crystalline planes are absent, showing that the VO_2 nanowires in LBfilm have a well-defined (00l) crystal plane orientation. To investigate the cause of orientation, we deposited LB film under low surface pressure, and the same phenomenon occurred, suggesting that the observed orientation was not caused by pressure. Meanwhile, we also observed the well-defined (00l) plane orientation of the transferred films of VO_2 nanowires functionalized only by SA. We speculate that the VO_2 nanowires on water subphase reorient, such that their (00l) crystal planes are parallel to the water–air interface, which results in the formation of oriented VO_2 nanowire LB film. During the transfer process, this ordered structure remains. Although the mechanism for (00l) plane orientation of VO_2 nanowire LB films is still open, we believe that monodispersed functionalization and resulting uniform distribution provide the possibility for the orientation of

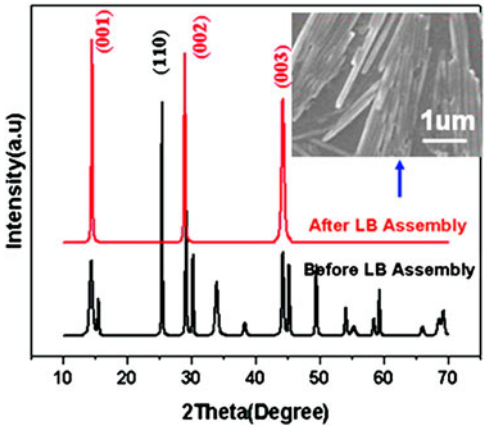

FIG. 3. XRD patterns of VO_2 nanowires before and after Langmuir-Blodgett (LB) assembly. Insert is the SEM image of VO_2 nanowire LB film.[31]

VO_2 nanowire LB film. Because the VO_2 nanowire surface has a large number of O-H bond and V-O bond groups, and the most closely packed (00l) crystal planes have the higher energy and more atoms, SA molecular and CTAB-SA complexes preferentially coordinate to the (001) surface, thereby driving the orientation.

III. VANADIUM OXIDE NANOWIRES FOR Li-ION BATTERY APPLICATION

A. VO_2 nanowires

Vanadium dioxides (VO_2) have more than 10 known phases with different structural characteristics.[33] Among these phases, metastable VO_2 (B) has layered structure to accommodate the guest ion intercalation for Li-ion battery applications.[34] Recently, VO_2 (B) nanorods with high crystallinity and a rectangular cross-section were successfully synthesized using a simple hydrothermal route.[35] VO_2 (B) nanorods as the positive electrode exhibit a high initial discharge capacity of 605 mAh/g, and it is found that the good electrochemical performance is attributed to the intrinsic properties of crystalline VO_2 (B) nanostructures. Zhou et al.[36] synthesized VO_2 (B) nanorods with diameters of 80–250 nm via a poly ethylene glycol-assisted hydrothermal approach. The VO_2 (B) nanorods show an initial discharge capacity of 310 and 250 mAh/g in the 30th cycle in the potential range of 1–3.5 V. Bruce and coworkers[37] synthesized ultrathin (<10-nm diameter) VO_2 (B) nanowires by a simple hydrothermal reaction. The ultrathin wires are arranged in bundles within which the wires lie in the same direction. In contrast, the standard wires are not so arranged but exist as isolated wires. The standard nanowires exhibit lengths of several microns, whereas the ultrathin wires are several hundred nanometers in length. As shown in Fig. 4(a), the ultrathin wires exhibit a higher discharge capacity compared with the standard wires with either $LiPF_6$ or lithium bis(oxalate) borate (LiBOB) as electrolyte. The initial, 30th, and 50th discharge capacities are about 250, 180, and 170 mAh/g in $LiPF_6$, respectively. It is likely that this increased capacity corresponds to faster kinetics for the ultrathin wires, resulting from their smaller diameter, which leads to shorter diffusion pathways for Li^+ on intercalation. Our group has synthesized VO_2 (B) nanowires[38] via the rheological self-assembling method from V_2O_5 and CTAB. The cycling efficiency for the first 30 times exceeds 95.0% [Fig. 4(b)]. The initial and 30th discharge capacities are about 250 and 180 mAh/g, respectively, which are in the same level as the result of Bruce and coworkers.[37] In contrast to normal VO_2 (B) crystal material whose reversible capacity is approximately 160 mAh/g, VO_2 (B) nanowires possess better electrochemical property because of stable structure and high surface activity.

Electrochemistry of the VO_2 nanowires LB film has been investigated in our group. The 10th cycle efficiency Q_{10} of VO_2 nanowires film before and after LB assembly is 98 and 99%, respectively, which shows huge enhancement in cyclability compared with V_2O_5 xerogel film reported previously.[39] Before LB assembly, the current density after enlarging 400 times has the same orders of magnitude to that after LB assembly, which shows that the current density and specific capacity of VO_2 nanowires LB films are approximately two orders higher than those of the VO_2 nanowire film before LB assembly, which is attributed to the formation of VO_2 nanowire monolayers. Moreover, in the cyclic voltammogram curves before and after LB assembly, only one oxidation peak was recorded corresponding to a two electron-transfer process, which is different with non-Nernstian redox couples and slow rate for the charge-transfer reaction of V_2O_5 films confirmed by the observation of two oxidation peaks. These differences can be explained by taking into account orientated and locally ordered structure of VO_2 LB film, which is helpful to insertion or extraction and transfer of Li^+ ions and makes the process quicker and more reversible.

B. V_2O_5 nanowires

Recently, V_2O_5 nanowires have been extensively studied to improve their electrochemical properties because of the short diffusion distances for the Li ions, a high contact surface area among the active materials, conductive additives and electrolyte, and good flexibility for volume changes during the electrochemical cycling. During the discharge process, the structural transitions of crystalline V_2O_5 can be reflected in the discharge curve as three plateaus at 3.4, 3.2, and 2.3 V for the α/ε, ε/δ, and δ/γ two-phase regions, respectively. The irreversible ω-$Li_3V_2O_5$ will form at a deeper discharge state.[13] Whittingham and coworkers[12] presented the evolution of the cycling ability of V_2O_5 with morphology changing from microcrystalline to nanocrystalline based on their own group's results. The

best capacity and cycling stability were demonstrated by the V_2O_5 nanorods synthesized by the annealing of $H_xV_4O_{10}{\cdot}nH_2O$ nanorods in oxygen. Recently, Whittingham and coworkers[25] found that the electrospun V_2O_5 nanofibers have a remarkably high discharge capacity, approaching 360 mAh/g in the first cycle and above 240 mAh/g after 25 cycles, as shown in Fig. 5(a). But there is a slight overcharge on each cycle when battery is cycled galvanostatically between 1.75 and 4.0 V, which is associated with reaction with the electrolyte. This is solved by the addition of a small amount of LiBOB to the electrolyte $LiPF_6$, leading to a more effective protective layer to improve the columbic efficiency close to 100%, but there is a loss in the capacity of the vanadium oxide.

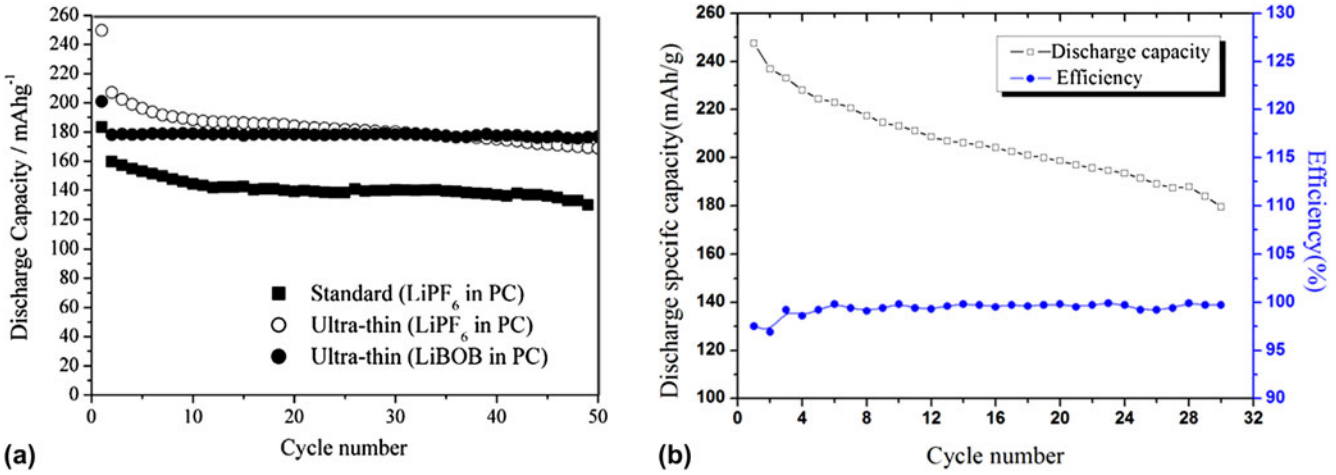

FIG. 4. (a) Discharge capacity versus cycle number for VO_2 (B) nanowires in $LiPF_6$ and lithium bis(oxalate)borate (LiBOB).[37] (b) Discharge specific capacity and efficiency versus cycling number for VO_2 (B) nanowires.[38]

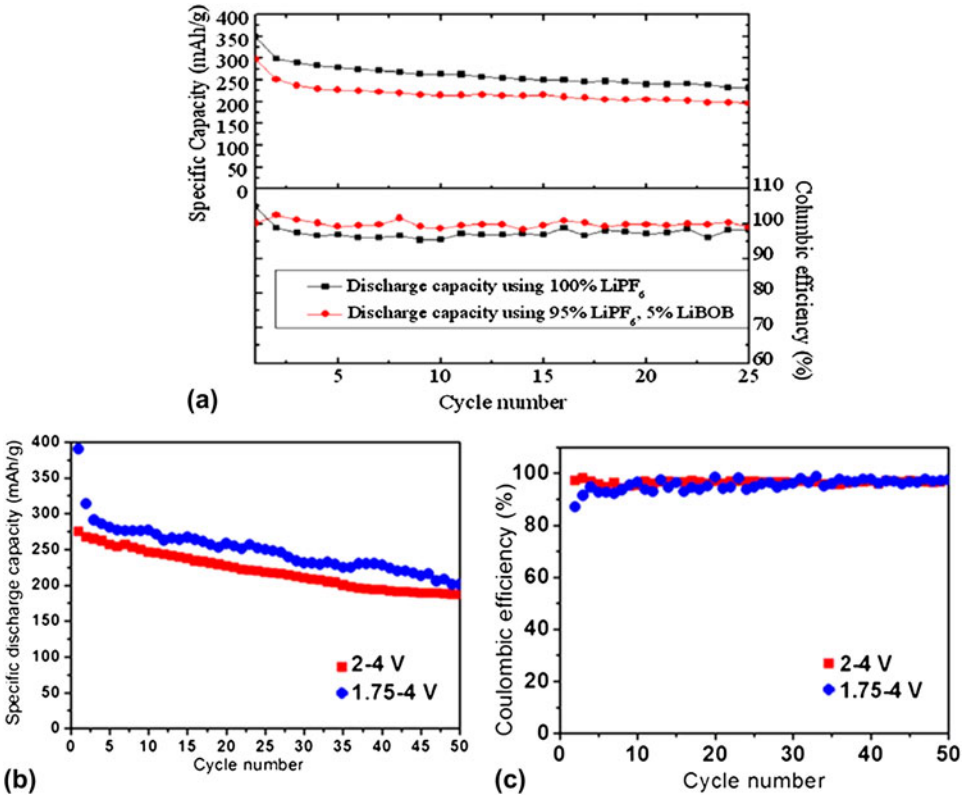

FIG. 5. (a) Capacity and cycling efficiency versus cycle number of nano-V_2O_5 using a pure $LiPF_6$ electrolyte solution and one containing 5% LiBOB.[25] (b) and (c) Capacity versus cycle number and coulombic efficiency versus cycle number of the ultralong hierarchical vanadium oxide nanowires.[28]

Chou et al.[40] synthesized V_2O_5 nanoribbons by an ultrasonic-assisted hydrothermal method combined with a postannealing process. Interestingly, the nanoribbons are composed of small nanoflakes. The nanoparticle has a porous structure on the surface with diameters less than 5 nm, which accounts for the high surface area. They reported that the possible reason for the formation of the pores is that the surfactant (Brij 30) could etch the surface of the raw V_2O_5 materials and show a surface porous structure after annealing. Owing to high surface area, porous V_2O_5 nanoribbons show the best capacity of 430 mAh/g for initial discharge, the best cyclability (270 mAh/g for the 50th cycle), good high-rate capability (119 mAh/g at 2 C current density). The room temperature ionic liquid electrolyte used in their work can prevent the dissolution of V_2O_5 during charge and discharge. Cui and coworkers[41] synthesized V_2O_5 nanoribbons by a chemical vapor transport method and studied Li-ion insertion in single V_2O_5 nanoribbon via chemical lithiation with n-BuLi. They found that the transformation of α-V_2O_5 into the δ-$Li_3V_2O_5$ phase depends not only on the width but also on the thickness of the nanoribbons. The transformation can take place within 10 s in thin nanoribbons, suggesting a Li^+ diffusion constant three orders of magnitude faster than in bulk materials, resulting in a significant increase in battery power density (360 C). Meanwhile, efficient electronic transport can be maintained to charge a $Li_3V_2O_5$ nanoribbon within less than 5 s. The V_2O_5 nanobelt array mentioned above exhibits greatly improved rate capability and cyclability, presenting a superior candidate for Li-ion batteries cathodes.[23] By regularly changing the current densities from 4000 to 1000, 400, and finally back to 4000 mA/g, they can observe the reversible capacity delivered from 150 to 180, 230, and then back to 150 mAh/g subsequently. When the V_2O_5 nanobelt array is tested as an anode in Li-ion batteries, the excellent electrochemical performance is achievable as well. The excellent performance for V_2O_5 nanobelt arrays on Ti substrates serving as cathodes and anodes is believed to be based on their unique designed architecture, which can be applied to other active materials in Li-ion batteries. Electrospun mesoporous V_2O_5 nanofibers fabricated by Cao and coworkers display an enhanced Li-ion storage capacity, excellent cyclic stability, and reversibility.[27] The initial discharge capacity is 377 mAh/g at a high charge/discharge rate of up to 800 mA/g. The charge/discharge capacity of mesoporous V_2O_5 nanofibers decreases slowly before the 9th cycle, and then the charge/discharge process becomes very stable with a discharge capacity of 347 mAh/g in the 10th cycle and a loss rate of 0.78% per cycle, which is attributed to the unique structures allowing easy mass and charge transfer with sufficient freedom for volume change accompanying the Li-ion intercalation and deintercalation.

Li-ion battery performance of the ultralong hierarchical V_2O_5 nanowires prepared by electrospinning in our group was investigated.[28] As shown in Fig. 5(b), when the battery is cycled between 1.75 and 4.0 V, the initial and 50th discharge capacities are up to 390 and 201 mAh/g, respectively, but the coulombic efficiency is not stable because of the irreversible-phase transition at 1.9 V [Fig. 5(c)]. So while the battery is cycled between 2.0 and 4.0 V, the coulombic efficiency is close to 100% and more stable. But the initial and 50th discharge capacities of the vanadium oxide reduce to 275 and 187 mAh/g because of the narrower cycling range. The ultralong hierarchical nanowires exhibit high specific capacity and good cycling capability because of the unique structure shown in Fig. 2, which can effectively prevent self-aggregation of the nanowires to keep the surface area large and fully realize the advantage of nanostructured materials.

C. Hydrated vanadium oxides nanowires

$V_3O_7{\cdot}H_2O$ is one of the hydrated vanadium oxides containing V^{5+} and V^{4+} in a ratio of 2:1, which is of interest because of the layered structure and redox activity. The layered structure of $V_3O_7{\cdot}H_2O$ contains VO_6 octahedra and VO_5 trigonal bipyramids with vanadium oxidation states of +4 and +5, respectively. The water molecule is bound to the vanadium ion by replacing one of the oxygen atoms in the VO_6 octahedron and forms hydrogen bonds with the octahedral in the next layer. Qiao et al.[42] have synthesized $V_3O_7{\cdot}H_2O$ nanowires via hydrothermal treatment of commercial V_2O_5 powder at relatively low temperatures. The synthetic process is free of any templates and reducing agents. The resulting $V_3O_7{\cdot}H_2O$ nanowires are 100–500 nm in width, several tens to several hundreds micrometers in length, and about 20 nm in average thickness. The typical width:thickness ratios were about 5–20. They reported that the $V_3O_7{\cdot}H_2O$ nanowires exhibited an initial high discharge specific capacity of 253.0 mAh/g in the potential range of 3.8–1.7 V, and the stabilized capacity still remained at 228.6 mAh/g after 50 cycles. Gao et al.[43] have synthesized single-crystal $V_3O_7{\cdot}H_2O$ nanobelts using a simple hydrothermal route. The synthesized nanobelts are highly crystalline and have lengths up to several tens of micrometers. The thickness and width of the nanobelts are found to be about 30 and 50 nm, respectively. The Li-ion battery using $V_3O_7{\cdot}H_2O$ nanobelts as the positive electrode exhibits a high initial discharge capacity of 409 mAh/g, corresponding to an intercalation of 4.32 mol Li^+ into 1 mol $V_3O_7{\cdot}H_2O$, which is a really high ratio of Li^+ to vanadium oxide. This outstanding performance can be attributed to the intrinsic characteristics of the single-crystalline $V_3O_7{\cdot}H_2O$ nanobelts. Zhang et al.[44] synthesized single-crystal $V_3O_7{\cdot}H_2O$ nanobelts in a large scale by ethanol reducing of the commercial V_2O_5 powder via a facile hydrothermal approach. The as-prepared $V_3O_7{\cdot}H_2O$ nanobelts are up to several tens of micrometers

in length, about 100 nm in width, and about 20 nm in thickness in average, respectively. The $V_3O_7{\cdot}H_2O$ nanobelts exhibit an initial discharge capacity of as high as 373 mAh/g in a voltage range of 4.0–1.5V and under a constant current density of 0.2 mA/cm^2. The high discharge capacity might be attributed to the large surface area and short diffusion distance resulting from the nanostructures. These results indicate that the $V_3O_7{\cdot}H_2O$ nanowires are promising cathode materials in Li-ion batteries.

In addition to $V_3O_7{\cdot}H_2O$ nanowires, the application in Li-ion batteries of some other hydrated vanadium oxides nanomaterials has also been investigated. Xie and coworkers [45] synthesized one-dimensional $V_2O_5{\cdot}0.6H_2O$ and $V_2O_5{\cdot}0.9H_2O$ nanorolls on a large scale by a simple hydrothermal growth route using NH_4VO_3 as the raw material. The initial discharge capacity of $V_2O_5{\cdot}0.6H_2O$ and $V_2O_5{\cdot}0.9H_2O$ nanorolls are 253.6 and 223.9 mAh/g, respectively. Moreover, the capacities of the annealed samples are higher than their hydrous precursors, which was 307.5 mAh/g for the annealed $V_2O_5{\cdot}0.6H_2O$ and 287.8 mAh/g for the annealed $V_2O_5{\cdot}0.9\ H_2O$. This result indicated that the interstitial water molecules in $V_2O_5{\cdot}xH_2O$ samples occupy some interlayer space of the structure and the spaces for the Li intercalation/deintercalation decrease, leading to a low charge–discharge capacity. Interestingly, this conclusion is different from a former one, which said that the expansion of V_2O_5 layers by water molecules could facilitate enhanced Li-ion intercalation performance of $V_2O_5{\cdot}xH_2O$.[46] These demonstrate that vanadium oxide nanomaterials with diverse morphologies will offer great opportunities for exploring the morphology dependence of the Li properties of a nanomaterial on its Li-ion intercalation performance for Li-ion battery applications.[14]

D. Other vanadium oxides nanowires

Besides the typical vanadium oxides, some other vanadium oxides nanowires have also drew much attention for Li-ion battery application, such as LiV_3O_8, $Li_xV_2O_5$, NaV_6O_{15}, and SVO. Liu et al.[47] have prepared LiV_3O_8 nanorods with highly crystalline and a single phase; the electrochemical performance of LiV_3O_8 nanorods was investigated, which demonstrated that as-prepared LiV_3O_8 nanorods exhibited as high as 348 mAh/g discharge capacity in first cycle at 20 mA/g current density and still remained at 303 mAh/g at 50 mA/g afterward; moreover, until 50 cycles, they kept 315 mAh/g, recorded at 50 mA/g. Sakunthala et al.[48] synthesized the LiV_3O_8 rods by the surfactant-assisted polymer precursor method, which delivered a discharge capacity of 230($\pm$5) mAh/g at the end of the second cycle, with an excellent capacity retention of 99.52% at the end of the 20th cycle, for a current density of 30 mA/g. LiV_3O_8 nanorods delivered a discharge capacity of 135($\pm$5) mAh/g at the end of 350 cycles, for a current density of 240 mA/g, and reasonably high capacity values were achieved at the different current rates. Semenenko et al.[49] showed the synthesis of single-crystalline $Li_xV_2O_5$ nanobelts, which drastically enhanced initial discharge specific capacity of 490 mAh/g and great cyclability. The capacity was maintained above 400 mAh/g for 50 cycles. Liu et al.[50] introduced a simple method to prepare highly crystallined single-phase NaV_6O_{15} nanorods. When used as the cathode material in rechargeable Li batteries, the NaV_6O_{15} nanorods exhibited stable Li-ion insertion/deinsertion reversibility and delivered as high as 328 mAh/g Li cycled at the current density of 0.02 A/g. In galvanostatic cycling test, a specific discharge capacity of approximately 300 mAh/g could be demonstrated for 70 cycles under 0.05 A/g current density.

SVO have been found ideally suitable for battery applications owing to their excellent electrochemical properties resulting from the variety of oxidation state of silver and vanadium. Among SVO, $Ag_2V_4O_{11}$ has been studied most, and it has demonstrated commercial success as a solid-state cathode material in primary Li power sources for implantable biomedical devices, such as the implantable cardiac defibrillator.[51] Another important stable-phase SVO is β-$AgVO_3$, whose electrochemical property highly depends on the composition, size, shape, crystal structure, and surface properties of the product. Zhu and coworkers[52] synthesized β-$AgVO_3$ nanowires with diameter of 30–60 nm and length of 1.5–3 μm by a simple and facile low-temperature sonochemical route. Cyclic voltammetry and charge–discharge experiments were applied to characterize the electrochemical properties of the nanowires as cathode materials for Li-ion batteries. The as-prepared β-$AgVO_3$ nanowires showed the initial charge and discharge capacities of 69 and 102 mAh/g, respectively. Zhang et al.[53] prepared β-$AgVO_3$ nanowires with diameter around 50 nm and length of several tens of micrometers via a simple and facile low-temperature hydrothermal approach. Electrochemical measurements of primary Li-ion batteries showed that the electrodes with the as-prepared β-$AgVO_3$ nanowires exhibited high discharge capacities of 302.1 mAh/g.

The battery property researches of SVO have mainly focused on primary Li-ion batteries. Recently, our group synthesized β-$AgVO_3$ nanowires [Fig. 6(a)] by rheological self-assembling process and investigated their rechargeable Li-ion battery property. To improve its electrochemical property, $AgVO_3$-PPy nanocables were then constructed using as-prepared $AgVO_3$ by in situ polymerization method.[54] $AgVO_3$-PPy nanocables can keep one-dimensional structure well, while the surface has become rough. The thickness of the PPy layer is about 6 nm [Figs. 6(c) and 6(d)].

It is found that the $AgVO_3$-PPy hybrid nanocables exhibit higher discharge capacity, capacity retention, and better cycling stability compared with the pristine β-$AgVO_3$ nanowires [Fig. 6(b)], resulting from the improvement of

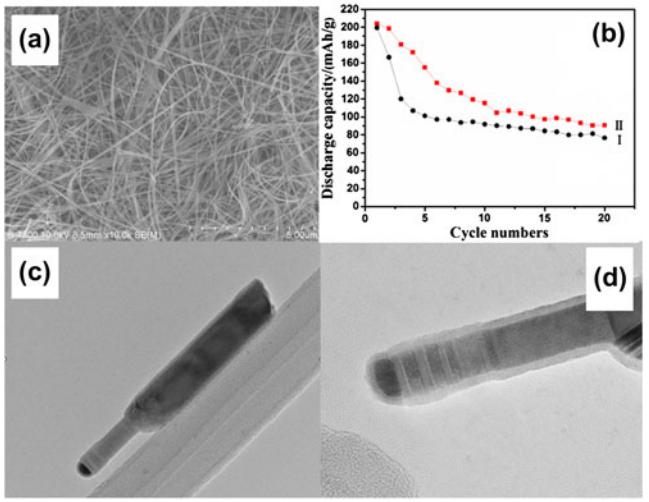

FIG. 6. (a) Typical FESEM image of the β-$AgVO_3$ nanowires. (b) Cyclability of the batteries assembled with the β-$AgVO_3$ nanowires (I) and the $AgVO_3$-PPy nanocables(II). (c) and (d) Typical TEM images of $AgVO_3$ and $AgVO_3$/PPy nanocable, respectively.[54]

electrical conductivity because of hybrid polymerization of pyrrole accompanied by change of band structure and carrier density. Furthermore, PPy can accommodate Li ions. When the β-$AgVO_3$ nanowires are enwrapped and interconnected with PPy coatings, the coated PPy layer could provide a fine pathway for electron transfer in the Li^+ ions insertion/extraction process. Thus, PPy facilitates the interfacial charge transfer and improves the utilization of the composite electrode, finally improving the electrochemical performances of the nanocables.

IV. VANADIUM OXIDE NANOWIRE-BASED NANODEVICES

As typical building blocks, vanadium oxide nanowires have been constructed into nanodevices to facilitate various applications in recent years, such as electrochromics, biological detections, photonic crystals, strain sensor, etc.[55–63]

Single nanostructure devices have been exploited to demonstrate a powerful diagnostic tool, which allows for the direct correlation of the electrochemical property with the structure on the same nanoscale particle.[64–69] Recently, our group has fabricated a single nanowire electrochemical device using $V_3O_7{\cdot}H_2O$ nanowire to investigate the fundamental mechanisms of capacity fading and the direct relationship between electrical transport, structure, and electrochemistry of vanadium oxide.[70] The device was configured with one nanowire as cathode, one flake of highly ordered pyrolytic graphite (HOPG) as counter electrode, and PEO, $LiClO_4$, and propylene carbonate as solid electrolytes [Fig. 7(a)].

This single nanowire battery design provides a unique platform for in situ probing the direct correlation of nanowire's electrical transport, structure, and electrochemistry

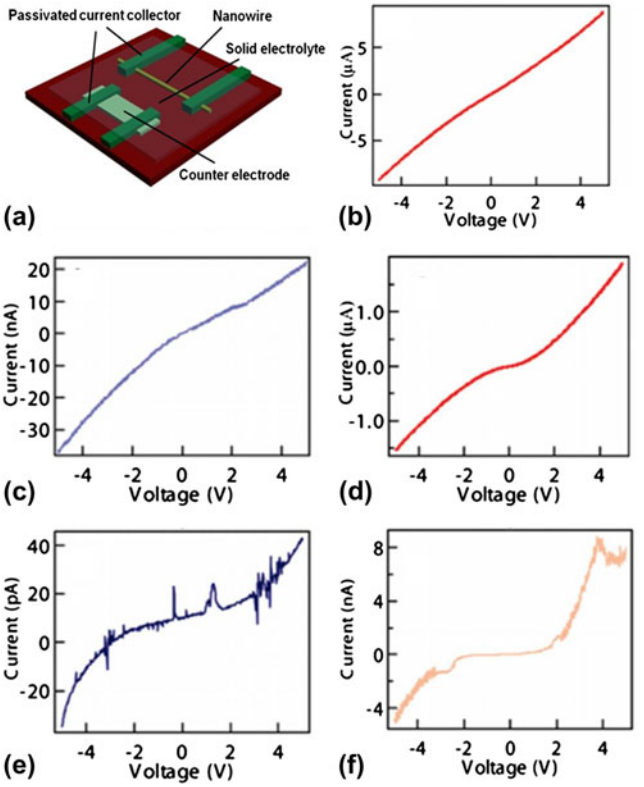

FIG. 7. (a) Schematic diagram of a single nanowire electrode device design. A single vanadium oxide nanowire is the work electrode, and HOPG nanofilm is the counter electrode. The electrolyte is the PEO-$LiClO_4$-PC-EC polymer. (b)–(f) Single vanadium oxide nanowire transport properties at different charge/discharge states are shown: (b) initial state; (c) after Li^+ ion intercalation (shallow discharge with 100 pA for 200 s); (d) after Li^+ ion deintercalation (shallow charge with −100 pA for 200 s); (e) after deep discharge with 100 pA for 400 s; and (f) after deep charge with −100 pA for 400 s.[70]

without disturbing the battery components. Figures 7(b)–7(f) show the transport properties of the same single nanowire at different charge/discharge status. Initially, the vanadium oxide nanowire is highly conductive [Fig. 7(b)], agreeing with its original intact crystal structures. Along with Li-ion intercalation by shallow discharge with 100 pA for 200 s, the nanowire conductance is decreased over two orders [Fig. 7(c)]. The conductance change can be restored to previous scale upon Li^+ ion deintercalation with shallow charge with −100 pA for 200 s [Fig. 7(d)] indicating reversible structure change. However, when the battery device is deeply discharged with 100 pA for 400 s, the nanowire conductance drops over five orders [Fig. 7(e)]. This change is permanent and could not be recovered even after deep charging with −100 pA for 400 s [Fig. 7(f)], indicating that permanent structure change happens when too many Li ions are intercalated into the vanadium oxide layered structures. Here, the material electrical properties, crystal structure change, and electrochemical charge/discharge status are clearly correlated on the single nanowire electrode platform.

V. CONCLUSIONS

Vanadium oxides have high capacities of about 300–650 mAh/g, which are considered as one of the most promising cathode materials for Li-ion battery. Nanowire cathodes are found to have excellent battery performance especially at high rate, because they have higher surface area, shorter Li^+ ion diffusion distances, and facile strain relaxation on electrochemical cycling. Therefore, vanadium oxide nanowires have the maximum potential for Li-ion battery application, especially for delivering high specific capacity at high discharge rates. As exemplified in this review, the researches of vanadium oxide nanowires have made great progress in not only the synthesis and construction methods but also the single nanowire electrochemical device and the application for Li-ion battery.

Our group has prepared vanadium oxide nanowires with improved Li-ion battery performance using rheological self-assembling, LB assembly, electrospinning, etc. VO_2 (B) nanowires synthesized via rheological self-assembling method exhibit much higher specific capacity than normal VO_2 (B) crystal material. The specific capacity of VO_2 nanowires LB films are approximately two orders higher than those of the VO_2 nanowire film before LB assembly, which is attributed to the formation of oriented VO_2 nanowire monolayers. Ultralong hierarchical V_2O_5 nanowires prepared by electrospinning have high specific capacity and stable cycling performance, which are supposed to result from the reduced self-aggregation of V_2O_5 nanowires. Moreover, we assembled a single nanowire electrochemical device using $V_3O_7{\cdot}H_2O$ nanowire, on which the material electrical properties, crystal structure change, and electrochemical charge/discharge status are clearly correlated. This article gives a summary of recent advances and our group's results of vanadium oxide nanowires' application in Li-ion battery, which can be helpful for their further researches and applications. Considering that vanadium oxides possess typical layered structure and versatile redox-dependent properties, one can foresee the tremendous possibility and potential of constructing high-performance, multifunctional, and hybrid nanodevices based on vanadium oxide nanowires for energy storage and self-powered nanosystem.

ACKNOWLEDGMENTS

This work was supported by the National Nature Science Foundation of China (50702039 and 51072153), Program for New Century Excellent Talents in University (NCET-10-0661), Self-Determined and Innovative Research Funds of SKLWUT and the Fundamental Research Funds for the Central Universities (2010-II-016). We thank Prof. C.M. Lieber of Harvard University, Prof. Z.L. Wang of Georgia Institute of Technology, Dr. Y.J. Dong, and Prof. Y. Shao of Massachusetts Institute of Technology for stimulating discussions and effective collaborations.

REFERENCES

1. J.B. Goodenough: Cathode materials: A personal perspective. *J. Power Sources* **174**, 996 (2007).
2. M. Ma, N.A. Chernova, B.H. Toby, P.Y. Zavalij, and M.S. Whittingham: Structural and electrochemical behavior of $LiMn_{0.4}Ni_{0.4}Co_{0.2}O_2$. *J. Power Sources* **165**, 517 (2007).
3. X. Ji, K.T. Lee, and L.F. Nazar: A highly ordered nanostructured carbon–sulphur cathode for lithium–sulphur batteries. *Nat. Mater.* **8**, 500 (2009).
4. R. Enjalbert and J. Galy: A refinement of the structure of V_2O_5. *Acta Crystallogr. C* **42**, 1469 (1986).
5. M.S. Whittingham: Lithium batteries and cathode materials. *Chem. Rev.* **104**, 4271 (2004).
6. M. Ganesan: Studies on the effect of titanium addition on $LiCoO_2$. *Ionics* **15**, 609 (2009).
7. P. Yang and C.M. Lieber: Nanorod-superconductor composites: A pathway to high critical current density materials. *Science* **273**, 1836 (1996).
8. D.K. Kim, P. Muralidharan, H.W. Lee, R. Ruffo, Y. Yang, C.K. Chan, H.L. Peng, R.A. Huggins, and Y. Cui: Spinel $LiMn_2O_4$ nanorods as lithium ion battery cathodes. *Nano Lett.* **8**, 3948 (2008).
9. H.W. Lee, P. Muralidharan, R. Ruffo, C.M. Mari, Y. Cui, and D.K. Kim: Ultrathin spinel $LiMn_2O_4$ nanowires as high power cathode materials for Li-ion batteries. *Nano Lett.* **10**, 3852 (2010).
10. E. Hosono, H. Matsuda, T. Saito, T. Kudo, M. Ichihara, I. Honma, and H.S. Zhou: Synthesis of single crystalline $Li_{0.44}MnO_2$ nanowires with large specific capacity and good high current density property for a positive electrode of Li ion battery. *J. Power Sources* **195**, 7098 (2010).
11. M.S. Whittingham: The role of ternary phases in cathode reactions. *J. Electrochem. Soc.* **123**, 315 (1976).
12. N.A. Chernova, M. Roppolo, A.C. Dillonb, and M.S. Whittingham: Layered vanadium and molybdenum oxides: Batteries and electrochromics. *J. Mater. Chem.* **10**, 2526 (2009).
13. Y. Wang and G.Z. Cao: Synthesis and enhanced intercalation properties of nanostructured vanadium oxides. *Chem. Mater.* **18**, 2787 (2006).
14. C.Z. Wu and Y. Xie: Promising vanadium oxide and hydroxide nanostructures: From energy storage to energy saving. *Energy Environ. Sci.* **3**, 1191 (2010).
15. T.Y. Zhai, H.M. Liu, H.Q. Li, X.S. Fang, M.Y. Liao, L. Li, H.S. Zhou, Y. Koide, Y. Bando, and D. Golberg: Centimeter-long V_2O_5 nanowires: From synthesis to field-emission, electrochemical, electrical transport, and photoconductive properties. *Adv. Mater.* **22**, 2547 (2010).
16. M.H. Kim, B. Lee, S. Lee, C. Larson, J.M. Baik, C.T. Yavuz, S. Seifert, S. Vajda, R.E. Winans, M. Moskovits, G.D. Stucky, and A.M. Wodtke: Growth of metal oxide nanowires from supercooled liquid nanodroplets. *Nano Lett.* **9**, 4138 (2009).
17. K. Takahashi, S.J. Limmer, Y. Wang, and G.Z. Cao: Synthesis and electrochemical properties of single-crystal V_2O_5 nanorod arrays by template-based electrodeposition. *J. Phys. Chem. B* **108**, 9795 (2004).
18. Y. Cheng, T.L. Wong, K.M. Ho, and N. Wang: The structure and growth mechanism of VO_2 nanowires. *J. Cryst. Growth* **311**, 1571 (2009).
19. J.M. Velazquez and S. Banerjee: Catalytic growth of single-crystalline V_2O_5 nanowire arrays. *Small* **5**, 1025 (2009).
20. M.C. Wu and C.S. Lee: Field emission of vertically aligned V_2O_5 nanowires on an ITO surface prepared with gaseous transport. *J. Solid State Electrochem.* **182**, 2285 (2009).
21. A.Q. Pan, J.G. Zhang, Z.M. Nie, G.Z. Cao, B.W. Arey, G.S. Li, S.Q. Liang, and J. Liu: Facile synthesized nanorod structured vanadium pentoxide for high-rate lithium batteries. *J. Mater. Chem.* **20**, 9193 (2010).

22. A.M. Glushenkov, V.I. Stukachev, M.F. Hassan, G.G. Kuvshinov, H.K. Liu, and Y. Chen: A novel approach for real mass transformation from V_2O_5 particles to nanorods. *Cryst. Growth Des.* **8**, 3661 (2008).
23. Y. Wang, H.J. Zhang, W.X. Lim, J.Y. Lin, and C.C. Wong: Designed strategy to fabricate a patterned V_2O_5 nanobelt array as a superior electrode for Li-ion batteries. *J. Mater. Chem.* **21**, 2362 (2011).
24. C. Ban and M.S. Whittingham: Nanoscale single-crystal vanadium oxides with layered structure by electrospinning and hydrothermal methods. *Solid State Ionics* **179**, 1721 (2008).
25. C. Ban, N.A. Chernova, and M.S. Whittingham: Electrospun nano-vanadium pentoxide cathode. *Electrochem. Commun.* **11**, 522 (2009).
26. P. Viswanathamurthi, N. Bhattarai, H.K. Kim, and D.R. Lee: Vanadium pentoxide nanofibers by electrospinning. *Scr. Mater.* **49**, 577 (2003).
27. D.M. Yu, C.G. Chen, S.H. Xie, Y.Y. Liu, K. Park, X.Y. Zhou, Q.F. Zhang, J.Y. Li, and G.Z. Cao: Mesoporous vanadium pentoxide nanofibers with significantly enhanced Li-ion storage properties by electrospinning. *Energy Environ. Sci.* **4**, 858 (2011).
28. L.Q. Mai, L. Xu, C.H. Han, X. Xu, Y.Z. Luo, S.Y. Zhao, and Y.L. Zhao: Electrospun ultralong hierarchical vanadium oxide nanowires with high performance for Lithium ion batteries. *Nano Lett.* **10**, 4750 (2010).
29. D. Whang, S. Jin, Y. Wu, and C.M. Lieber: Large-scale hierarchical organization of nanowire arrays for integrated nanosystems. *Nano Lett.* **3**, 1255 (2003).
30. D. Whang, S. Jin, and C.M. Lieber: Nanolithography using hierarchically assembled nanowire masks. *Nano Lett.* **3**, 951 (2003).
31. L.Q. Mai, Y.H. Gu, C.H. Han, B. Hu, W. Chen, P.C. Zhang, L. Xu, W.L. Guo, and Y. Dai: Orientated Langmuir-Blodgett assembly of VO_2 nanowires. *Nano. Lett.* **9**, 826 (2009).
32. L.Q. Mai, W. Chen, Q. Xu, J.F. Peng, and Q.Y. Zhu: Low-cost synthesis of novel vanadium dioxide nanorods. *Int. J. Nanosci.* **3**, 225 (2004).
33. M.D. Wei, H. Sugihara, I. Honma, M. Ichihara, and H.S. Zhou: A new metastable phase of crystallized $V_2O_4{\cdot}0.25\ H_2O$ nanowires: Synthesis and electrochemical measurements. *Adv. Mater.* **17**, 2964 (2005).
34. J. Galy: Vanadium pentoxide and vanadium oxide bronzes—Structural chemistry of single (S) and double (D) layer $M_xV_2O_5$ phases. *J. Solid State Chem.* **100**, 229 (1992).
35. Z.J. Chen, S.K. Gao, L.L. Jiang, M.D. Wei, and K.M. Wei: Crystalline VO_2 (B) nanorods with a rectangular cross-section. *Mater. Chem. Phys.* **121**, 254 (2010).
36. F. Zhou, X.M. Zhao, H. Xu, and C.G. Yuan: Hydrothermal synthesis of metastable VO_2 nanorods as cathode materials for lithium ion batteries. *Chem. Lett.* **11**, 1280 (2006).
37. G. Armstrong, J. Canales, A.R. Armstrong, and P.G. Bruce: The synthesis and lithium intercalation electrochemistry of VO_2 (B) ultra-thin nanowires. *J. Power Sources* **178**, 723 (2008).
38. W. Chen, L.Q. Mai, Y.Y. Qi, and Y. Dai: One-dimensional nanomaterials of vanadium and molybdenum oxides. *J. Phys. Chem. Solids*. **67**, 896 (2006).
39. W. Chen, Q. Xu, Y. Hu, L. Mai, and Q. Zhu: Effect of modification by poly (ethylene oxide)on the reversibility of insertion/extraction of Li^+ ion in V_2O_5 xerogel films. *J. Mater. Chem.* **12**, 1926 (2002).
40. S.L. Chou, J.Z. Wang, J.Z. Sun, D. Wexler, M. Forsyth, H.K. Liu, D.R. MacFarlane, and S.X. Dou: High capacity, safety, and enhanced cyclability of lithium metal battery using a V_2O_5 nanomaterial cathode and room temperature ionic liquid electrolyte. *Chem. Mater.* **20**, 7044 (2008).
41. C.K. Chan, H. Peng, R.D. Twesten, K. Jarausch, X.F. Zhang, and Y. Cui: Fast, completely reversible Li insertion in vanadium pentoxide nanoribbons. *Nano Lett.* **7**, 490 (2007).
42. H. Qiao, X. Zhu, Z. Zheng, L. Liu, and L. Zhang: Synthesis of $V_3O_7{\cdot}H_2O$ nanobelts as cathode materials for lithium–ion batteries. *Electrochem. Commun.* **8**, 21 (2006).
43. S.K. Gao, Z.J. Chen, M.D. Wei, K.M. Wei, and H.S. Zhou: Single crystal nanobelts of $V_3O_7{\cdot}H_2O$: A lithium intercalation host with a large capacity. *Electrochim. Acta* **54**, 1115 (2009).
44. Y.F. Zhang, X.H. Liu, G.Y. Xie, L. Yu, S.P. Yi, M.J. Hu, and C. Huang: Hydrothermal synthesis, characterization, formation mechanism and electrochemical property of $V_3O_7{\cdot}H_2O$ single-crystal nanobelts. *Mater. Sci. Eng., B* **175**, 164 (2010).
45. B.X. Li, Y. Xu, G.X. Rong, M. Jing, and Y. Xie: Vanadium pentoxide nanobelts and nanorolls: From controllable synthesis to investigation of their electrochemical properties and photocatalytic activities. *Nanotechnology* **17**, 2560 (2006).
46. V. Petkov, P.N. Trikalitis, E.S. Bozin, S.J.L. Billinge, T. Vogt, and M.G. Kanatzidis: Structure of $V_2O_5.nH_2O$ xerogel solved by the atomic pair distribution function technique. *J. Am. Chem. Soc.* **124**, 10157 (2002).
47. H.M. Liu, Y.G. Wang, K.X. Wang, Y.R. Wang, and H.S. Zhou: Synthesis and electrochemical properties of single-crystalline LiV_3O_8 nanorods as cathode materials for rechargeable lithium batteries. *J. Power Sources* **192**, 668 (2009).
48. A. Sakunthala, M.V. Reddy, S. Selvasekarapandian, B.V.R. Chowdari, and P. Christopher Selvin: Preparation, characterization, and electrochemical performance of lithium trivanadate rods by a surfactant-assisted polymer precursor method for lithium batteries. *J. Phys. Chem. C* **114**, 8099 (2010).
49. D.A. Semenenko, D.M. Itkis, E.A. Pomerantseva, E.A. Goodilin, T.L. Kulova, A.M. Skundin, and Y.D. Tretyakov: $Li_xV_2O_5$ nanobelts for high capacity lithium-ion battery cathodes. *Electrochem. Commun.* **12**, 1154 (2010).
50. H.M. Liu, Y.G. Wang, L. Li, K.X. Wang, E. Hosono, and H.S. Zhou: Facile synthesis of NaV_6O_{15} nanorods and its electrochemical behavior as cathode material in rechargeable lithium batteries. *J. Mater. Chem.* **19**, 7885 (2009).
51. J.T. Kenneth, A.L. Randolph, J.P. Marcus, C.M. Amy, and S.T. Esther: Advanced lithium batteries for implantable medical devices: Mechanistic study of SVO cathode synthesis. *J. Power Sources* **119-121**, 973 (2003).
52. C.J. Mao, X.C. Wu, and J.J. Zhu: Large scale preparation of beta-$AgVO_3$ nanowires using a novel sonochemical route. *J. Nanosci. Nanotechnol.* **8**, 3203 (2008).
53. S.Y. Zhang, W.Y. Li, C.S. Li, and J. Chen: Synthesis, characterization, and electrochemical properties of $Ag_2V_4O_{11}$ and $AgVO_3$ 1-D nano/microstructures. *J. Phys. Chem. B* **110**, 24855 (2006).
54. Q. Gao, L.Q. Mai, L. Xu, Y.H. Gu, B. Hu, Y.L. Zhao, and J.H. Han: Construction and electrical transport properties of one-dimensional vanadium oxide nanomaterials. *Sciencepaper Online* **5**, 323 (2010).
55. K.C. Cheng, F.R. Chen, and J.J. Kai: V_2O_5 nanowires as a functional material for electrochromic device. *Sol. Energy Mater. Sol. Cells* **90**, 1156 (2006).
56. C.R. Xiong, A.E. Aliev, B. Gnade, and K.J. Balkus Jr.: Fabrication of silver vanadium oxide and V_2O_5 nanowires for electrochromics. *ACS Nano* **2**, 293 (2008).
57. W. Zhang, T. Yang, W.J. Li, G.C. Li, and K. Jiao: Rapid and sensitive electrochemical sensing of DNA damage induced by V_2O_5 nanobelts/HCl/H_2O_2 system in natural dsDNA layer-by-layer films. *Biosens. Bioelectron.* **25**, 2370 (2010).
58. A. Zylbersztejn and N.F. Mott: Metal-insulator transition in vanadium dioxide. *Phys. Rev. B* **11**, 4383 (1975).
59. D. Xiao, K.W. Kim, and J.M. Zavada: Electrically programmable photonic crystal slab based on the metal-insulator transition in VO_2. *J. Appl. Phys.* **97**, 106102 (2005).

60. D. Xiao, K.W. Kim, G. Lazzi, and J.M. Zavada: Tunable waveguiding in electrically programmable VO_2-based photonic crystals. *J. Appl. Phys.* **99**, 113106 (2006).
61. I.M. Povey, M. Bardosova, F. Chalvet, M.E. Pemble, and H.M. Yates: Atomic layer deposition for the fabrication of 3D photonic crystals structures: Growth of Al_2O_3 and VO_2 photonic crystal systems. *Surf. Coat. Tech.* **201**, 9345 (2007).
62. A.B. Pevtsov, D.A. Kurdyukov, V.G. Golubev, A.V. Akimov, A.A. Meluchev, A.V. Sel'kin, A.A. Kaplyanskii, D.R. Yakovlev, and M. Bayer: Ultrafast stop band kinetics in a three-dimensional opal- VO_2 photonic crystal controlled by a photoinduced semiconductor-metal phase transition. *Phys. Rev. B* **75**, 153101 (2007).
63. B. Hu, Y. Ding, W. Chen, D. Kulkarni, Y. Shen, V.V. Tsukruk, and Z.L. Wang: External-strain induced insulating phase transition in VO_2 nanobeam and its application as flexible strain sensor. *Adv. Mater.* **22**, 5134 (2010).
64. J.K. Campbell, L. Sun, and R.M. Crooks: Electrochemistry using single carbon nanotubes. *J. Am. Chem. Soc.* **121**, 3779 (1999).
65. I. Heller, J. Kong, H.A. Heering, K.A. Williams, S.G. Lemay, and C. Dekker: Individual single-walled carbon nanotubes as nanoelectrodes for electrochemistry. *Nano Lett.* **5**, 137 (2005).
66. Y. Yang, C. Xie, R. Ruffo, H.L. Peng, D.K. Kim, and Y. Cui: Single nanorod devices for battery diagnostics: A case study on $LiMn_2O_4$. *Nano Lett.* **9**, 4109 (2009).
67. Y. Yang, C. Xie, R. Ruffo, H.L. Peng, D.K. Kim, and Y. Cui: Single nanorod devices for battery diagnostics: A case study on $LiMn_2O_4$. *Nano Lett.* **9**, 4109 (2009).
68. J.Y. Huang, L. Zhong, C.M. Wang, J.P. Sullivan, W. Xu, L.Q. Zhang, S. Mao, N. Hudak, X.H. Liu, A.K. Subramanian, H. Fan, L. Qi, A. Kushima, and J. Li: In situ observation of the electrochemical lithiation of a single SnO_2 nanowire electrode. *Science* **330**, 1515 (2010).
69. C.M. Wang, W. Xu, J. Liu, D. Choi, B.W. Arey, L.V. Saraf, J. Zhang, Z. Yang, S. Thevuthasan, D.R. Baer, and N. Salmon: In-situ transmission electron microscopy and spectroscopy studies of interfaces in Li-ion batteries: Challenges and opportunities. *J. Mater. Res.* **25**, 1541 (2010).
70. L.Q. Mai, Y.J. Dong, L. Xu, and C.H. Han: Single nanowire electrochemical devices. *Nano Lett.* **10**, 4273 (2010).